D0 Note 3366, December 1997

Technical Design Report for the DØ Forward Muon Tracking Detector Based on Mini-drift Tubes

G. Alexeev, V. Anosov, Yu. Gornushkin, N. Jouravlev, A. Kalinin, E. Komissarov, V. Malyshev, Yu. Merekov, A. Nozdrin, I. Pisarev, N. Russakovich, B. Sabirov, V. Teterin, V. Tokmenin, L. Vertogradov, Yu. Yatsunenko
Joint Institute for Nuclear Research, Dubna

B. Baldin, E. Chi, D. Denisov, H.T. Diehl, D.R. Green, H. Haggerty, S. Hansen, A.S. Ito, N. Mokhov, G. Smith, A. Stefanik, R. Williams, F. Yoffe
Fermi National Accelerator Laboratory

J.M. Butler
Boston University

K. Davis, K. Johns
University of Arizona

D. Hedin, D. Beutel, J. Raskowski, V. Sirotenko
Northern Illinois University

Contents

1 Introduction

The goal of the DØ Upgrade [1] is to exploit the physics potential to be presented by the Main Injector and the Tevatron Collider during Run II. An integrated luminosity of 2 fb^{-1} is expected with an instantaneous luminosity of up to $2 \cdot 10^{32} cm^{-2}s^{-1}$ accompanied by a reduction in a bunch spacing. This order of magnitude increase in integrated luminosity over Run I will provide an opportunity for significant improvements in the wide range of physics studied at DØ during Run I.

The capability to identify and trigger on muons is one of the key features necessary to exploit these possibilties. Since studies of the aging of WAMUS chambers (the "EF" PDTs) reveal that these chambers will not survive Run II [2], a new design for the Forward Angle MUon System (FAMUS) has been developed.

The physics motivations for going to the highest luminosity are studies of low-cross-section, high-p_T processes, such as top and W/Z, and the search for new phenomena. It was shown [3] that $|\eta|$ coverage out to ~ 2 is important for high p_T physics. The Run II DØ muon system features full coverage for $|\eta| \lesssim 2$.

The proposed layout of the forward ($1.0 < |\eta| < 2.0$) muon system is presented in Fig. 1. It consists of the following major parts:

- 3 layers of Mini-drift Tubes (MDTs) for muon track reconstruction;
- 3 layers of scintillation counters for triggering on events with muons [4];
- Shielding around the beam pipe from calorimeter to the accelerator tunnel to reduce trigger rates, fake track reconstruction, and aging of detectors [5, 6, 7, 8, 9].

The detectors are arranged so that muons from the interaction point traverse three layers of MDTs: A, B, and C on both sides of the detector (see Fig.1). Layer A is closest to the inner surface of the magnet, layer B is near the outer surface of the magnet, and layer C is the most distant from the detector center. Three layers of MDTs will be used for muon identification and to complement the central tracking detector for muon momentum measurement with accuracy of σ_p/p =20% [10] for low momentum muons limited by multiple scattering in the muon toroid. MDTs will also be used to confirm muon trigger in the pseudorapidity region between 1.0 and 2.0. MDTs provide a set of considerable advantages for the DØ muon detector upgrade :

- maximum electron drift time below 132 ns bunch crossing time;
- coordinate resolution below 1 mm;
- high radiation hardness;
- high segmentation and low occupancy.

In this document we present the technical design of the FAMUS tracking system based on MDTs. Section 2 describes the design of MDT layers and individual tubes. Characteristics of MDTs are presented in Section 3. The high voltage system and electronics are described in

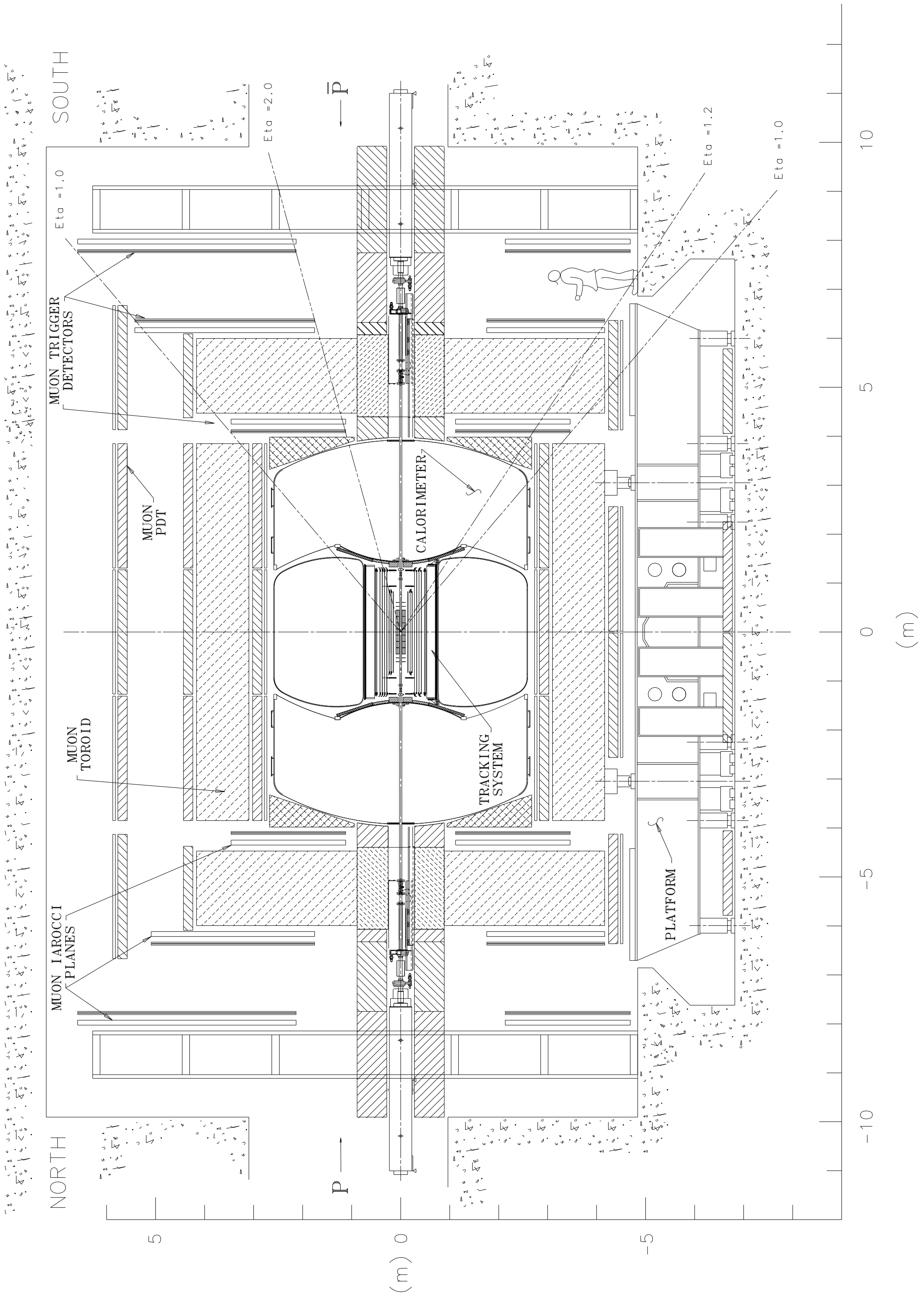

Figure 1: Side view of the DØ upgrade detector including various elements of the upgraded muon system.

Section 4. Section 5 describes the gas system and Section 6 presents our plans for alignment and survey. A description of assembly and commissioning in Section 7 is followed by a cost estimate and schedule in Section 8.

2 Forward Muon Tracking Detector

2.1 System Layout

Iarocci-type mini-drift tubes have been chosen as a coordinate detector for the forward muon system. Iarocci tubes have been extensively used in the high-energy physics experiments [11, 12] and are considered to be robust and reliable detector. We use the well developed technology of eight cell tube production existing at JINR with minor modifications (see below). The track position will be determined by drift time measurement with a coordinate accuracy of $\sigma_x \approx 0.7$ mm. To provide the necessary redundancy and track segment reconstruction capability, the tubes are arranged in layers (A, B and C) that consist of 3 or 4 planes (Fig. 2). The planes consist of tubes, and every tube has eight 1x1 cm^2 cells [13].

The layers (A, B or C) are divided into 8 octants. Each octant (Fig. 4) contains tubes of different lengths and is an independent assembly unit. Each MDT octant allows track segment reconstruction, providing information about both the position of a track and its direction. The planes are mounted on a support structure made of aluminium bars. From both sides MDT planes are covered with aluminum sheets which protect the detector from picking up noise (serving as a Faraday cage) and reduce the probability of track segment formation by low energy electrons. The efficiency of the aluminium absorber between MDT planes is presented in Fig. 3. The efficiency here is defined as a number of correlated hits in two planes without the absorber to the same value with the absorber. The studies have been done using GEANT 3.21 and GCALOR 1.04/09 simulation including low energy particle propagation. As most background hits are produced by electrons with energy ≤ 1 MeV, 1 g/cm^2 absorbers provide necessary shielding.

The layout of the MDT A-layer is shown in Fig. 4. The A-layer has a cut in the two bottom octants to accommodate the calorimeter support. The bottom octants of layers B and C are shorter than others because their size is restricted by the collision hall floor.

Table 1 summarizes the number of tubes, the eta coverage, and the number of readout channels for each layer.

Table 1: MDT system.

Layer	A	B	C
Number of tubes	2048	1944	2088
Number of readout channels	16384	15552	16704
η_{max}	2.15	2.13	2.16
η_{min}	0.996	1.022	1.13
Maximum tube length(mm)	3571	5066	5830

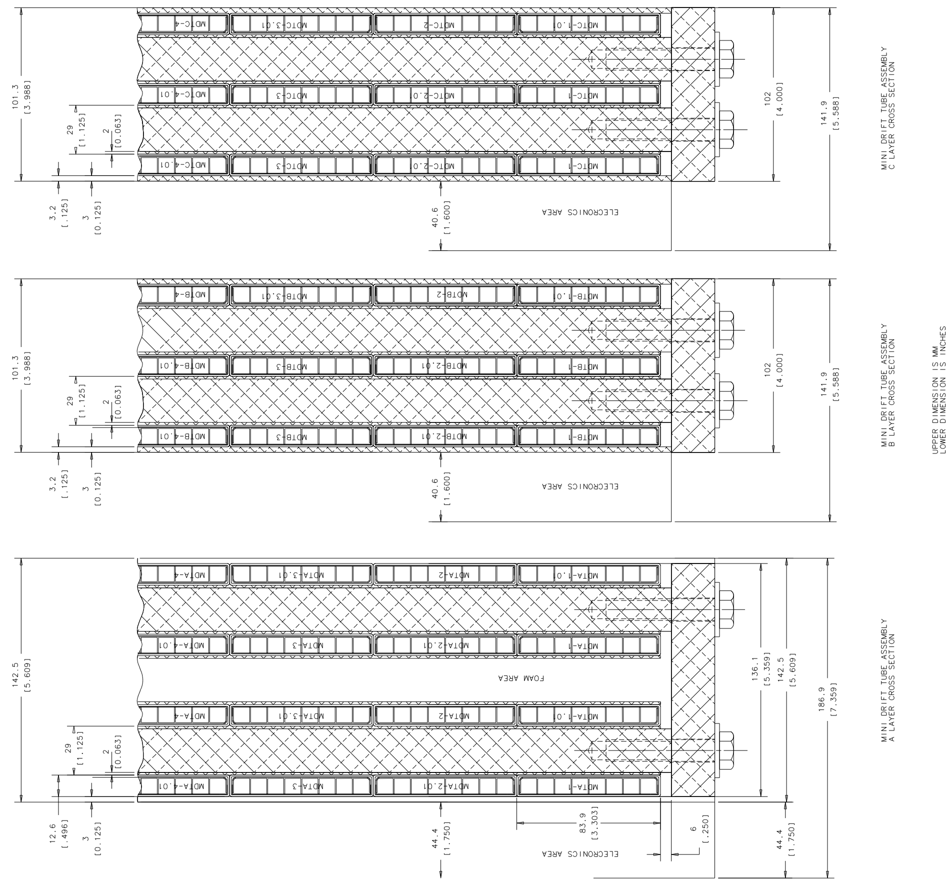

Figure 2: The layout of A, B and C layers.

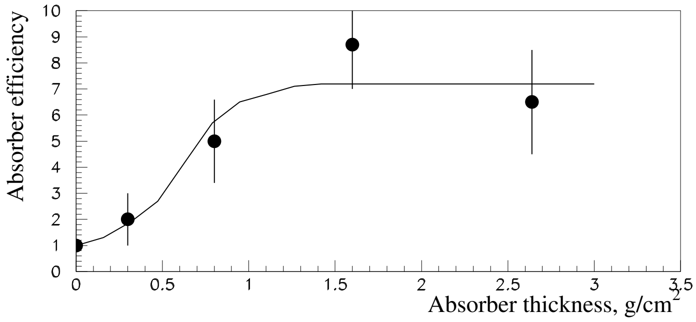

Figure 3: Efficiency of Al absorber between MDT planes

Layers A and B are mounted directly on the EF toroid. The C-layer will be installed on the EFC support structure.

The tubes are mounted along magnetic field lines (the field shape in EF toroid is more "square" than "circular"). The flux of particles drops with increasing distance from the beam pipe. Using the layer's geometry (Fig. 4), the occupancy of individual tubes will be the same over the entire layer within a factor of two. This geometry also minimizes number of channels per layer taking into account that tubes can be rather long (see Table 1).

2.2 Design of Individual 8 Cell Tube

An individual tube (Fig. 5, 6) consists of 8 cells, each with a 9.4×9.4 mm^2 internal cross section with a 50 μm (W-Au) anode wire in the center. The tubes are made from commercially available aluminium extrusion combs with stainless steel cover foil (0.15 mm thick) and inserted into plastic (PVC) sleeves with a length of up to 6 m and thickness 1 mm. The wall thickness of an aluminium comb is 0.6 mm.

The tubes are closed by endcaps that provide accurate positioning of the anode wires, wire tension, gas tightness, and electrical and gas connections. The mechanical tolerance on a wire position within a tube is 160μm, provided by automated assembly procedures and is well below the coordinate resolution of the MDT. One endcap has only a gas connector and the other has a gas connector, HV connector and individual signal connectors for 8 wires. Negative high voltage is applied to the cathode while the anode wire is grounded at the amplifier. Filled with a fast gas mixture (such as CF_4(90%)+CH_4(10%)), the MDT will provide a maximum electron drift time of about 60 ns. The proposed gate width of 100 ns is well within the 132 ns bunch spacing time. Table 2 summarizes the parameters of the individual MDTs.

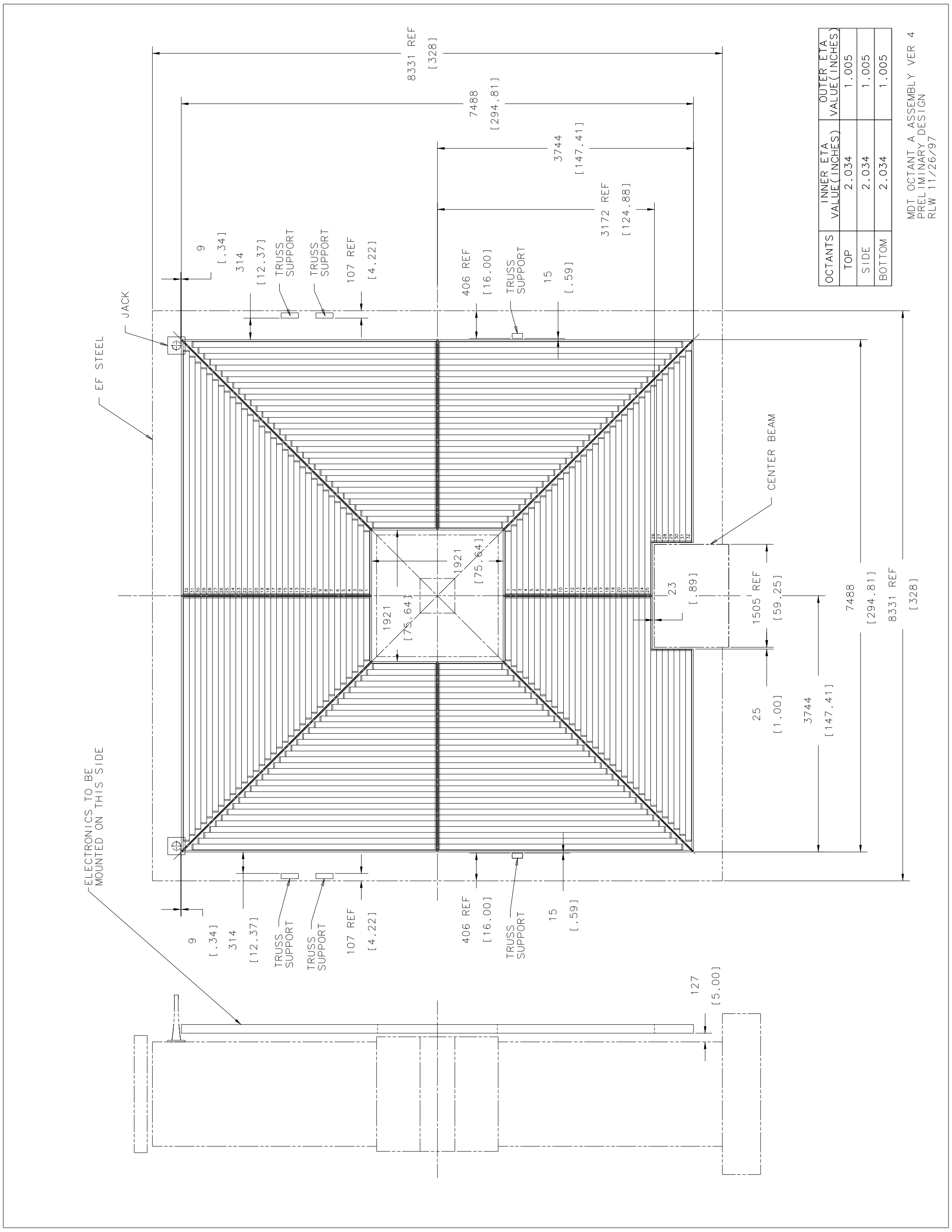

Figure 4: MDT A-layer design.

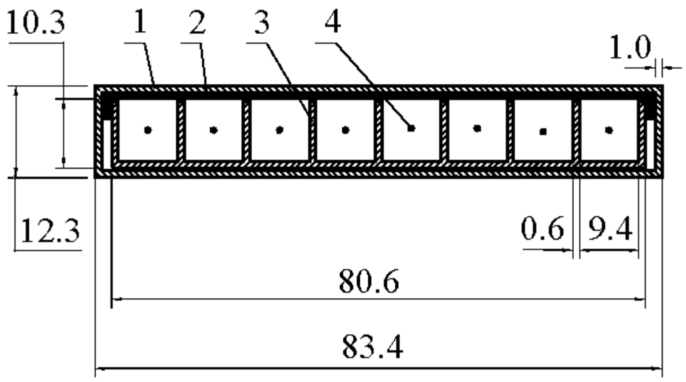

1 – envelope
2 – cover
3 – profile
4 – wires

Figure 5: Design of the 8 cell tube.

3 Mini-drift Tube Characteristics

3.1 Efficiency

The efficiency of Iarocci type tubes has been tested in numerous experiments and is approximately 100% in the active area of the cells for tracks perpendicular to the MDT plane. Due to the walls the actual efficiency is less and in our case is about 94% (the walls are 0.6 mm thick and the wire step is 10 mm). For inclined tracks, the effect of the walls is less important, and the efficiency of planes becomes 100%. The inclined tracks can cross two neighbouring cells in one MDT plane and, therefore, produce two hits per plane.

The MDT efficiency has been studied in a test beam at Fermilab. The 3.5 m long prototype was placed between two Proportional Wire Chambers (PWC) (reference system) so that the track position in the MDT module was known (the PWCs have 1 mm signal wire step). The efficiency of the MDTs has been studied for perpendicular and for inclined tracks at several points along the wire including a zone where wire supports are located. In Fig. 7, the efficiency for perpendicular tracks is presented. The efficiency goes down near the Al profile walls.

The efficiency near the spacers (wire supports) has been measured in the test beam. Due to electric field degradation, the efficiency goes down in a region of about 10 mm around the spacer (Fig. 8). The spacer size along the wire is 5 mm. The measured efficiencies can be used in MDT Monte Carlo simulation.

For inclined tracks the MDT layer can have more than one hit. For example, 45^0 tracks in the test beam produce one or two hits per layer (Fig. 9). The probability to have 2 hits in neighbouring cells depends on the track's entry point as is shown in Fig. 9.

To reconstruct a muon track segment, at least 2 hits per layer are needed. Taking into

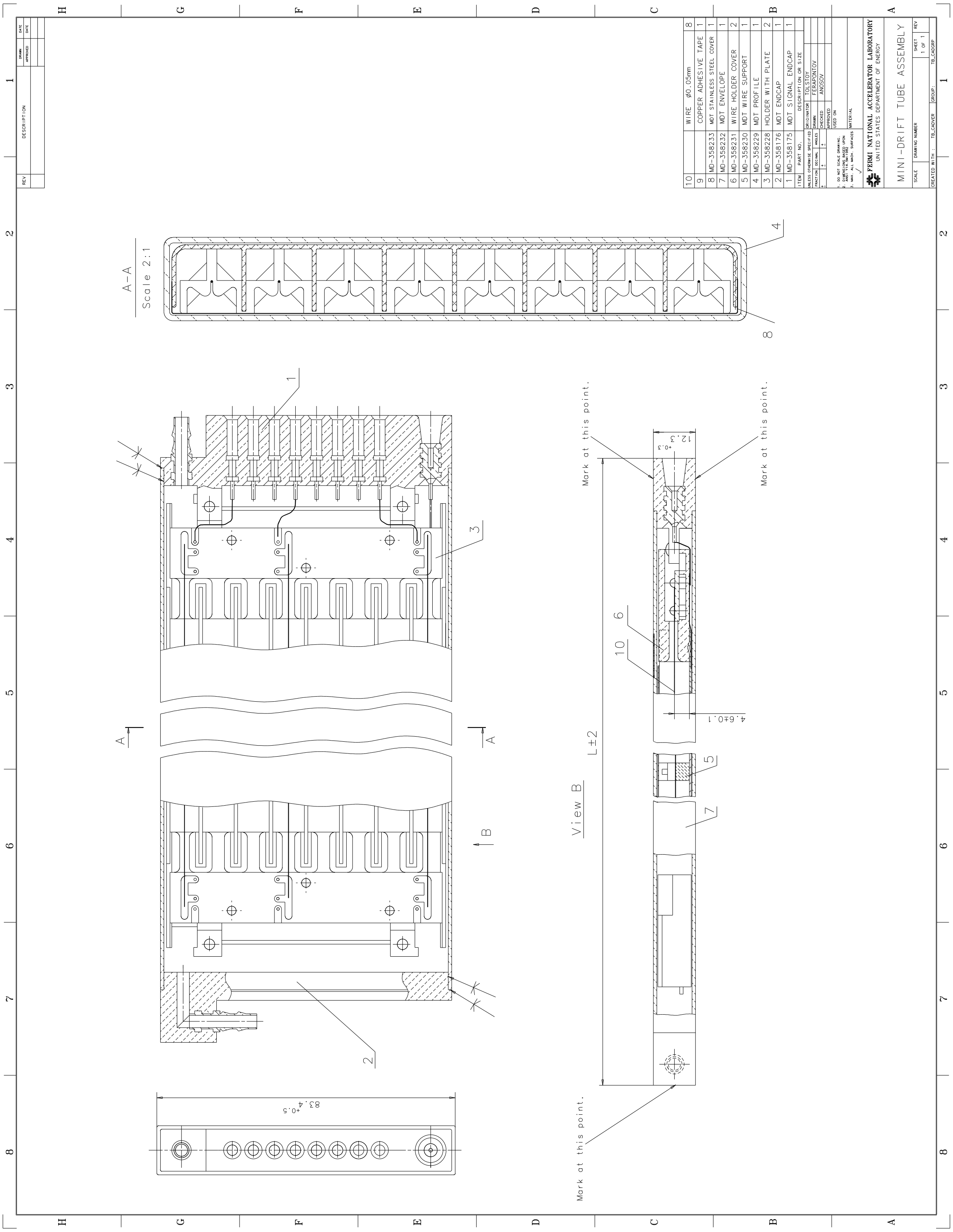

Figure 6: The assembly of the 8 cell tube.

Table 2: MDT parameters.

Wire step	10 mm
Wall thickness	0.6 mm
Cathode material	Al, stainless steel
Wire material	W-Au(96%:4%)
Wire diameter	50 μm
Gas mixture	CF_4(90%)+CH_4(10%)
Gas gain	2x10^5
Cathode potential	-3100 V
Maximum drift time	60 ns

account the 94% efficiency of one plane, the overall segment finding efficiency for 3 planes (the 2-out-of-3 efficiency) is 99%. the B and C layers contain 3 planes of MDTs, whereas the A-layer employs 4 MDT planes. The A-layer background flux is a factor of 3 higher than for the B and C layers. To detect soft muons (those ranging out in the EF toroid) at least 3 points are required on the track segment. Calculations show that even in the worst case of 94% single plane efficiency, the 3-out-of-4 efficiency is above 98%. The reasonably large number of points on track will improve the coordinate accuracy of the track reconstruction (by improving momentum resolution and the match with central detector tracks) and make track reconstruction algorithms more robust.

3.2 Dead Zones

Dead zones at the ends of the tubes produce 4% inefficiency for a 3 m long tube: 6 cm endcaps that consist of wire holders, HV, signal and gas connectors. The current design of the tubes keeps those dead zones at the lowest level taking into account reliability, safety and performance requirements. The gaps between the octants for mounting, gas connections, HV, and signal cables add 5% to the overall A layer inefficiency with an average tube length of 3 m. For the B and C layers, where the average length of MDT tubes is about 4 m, the dead zone due to the endcaps and gaps between octants is around 6%. The gaps between octants are at the same phi positions in all 3 layers, so the overall MDT detection efficiency is determined by A layer dead zones. The overall reconstruction efficiency of the FAMUS detector is around 90% [10].

3.3 Coordinate Resolution

The momentum resolution of the FAMUS spectrometer is limited by multiple scattering in the iron toroid and the coordinate resolution of the tracking detector. The typical coordinate resolution of WAMUS and SAMUS detectors in Run I was around 1 mm (per layer). Mechanical inaccuracies, survey, and time-to-distance calibration are the major factors limiting the resolution. In Section 6 the alignment and survey plans are discussed in details and Table 3 contains the alignment requirements. Taking into account those numbers and the

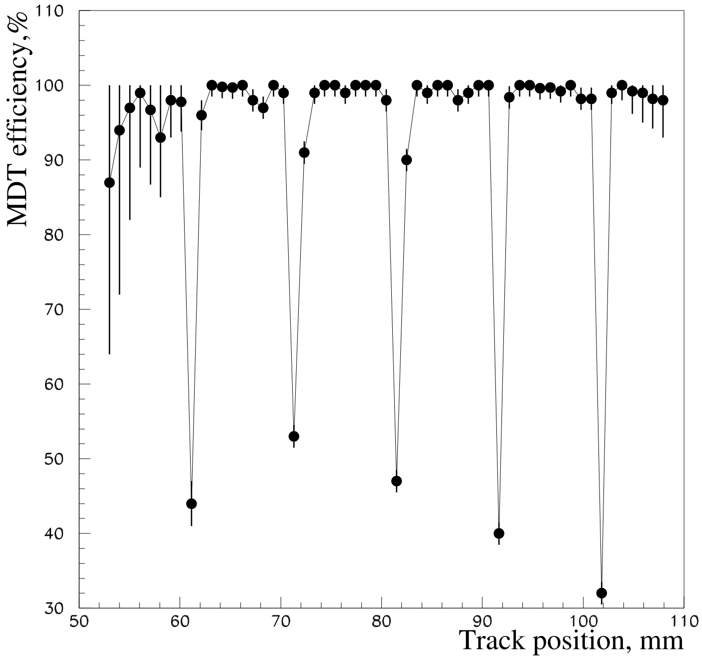

Figure 7: Detection efficiency of MDTs.

drift distance measurement accuracy (about 0.7 mm) due to the 18.8 ns time bin of digitizing electronics the overall track measurement resolution per plane will be about 0.9 mm. And the effective coordinate resolution per layer (with 3 or 4 planes) will be about 0.7 mm.

Taking into account the coordinate resolution, the magnetic field in the EF toroid, multiple scattering, and the layout of the planes, FAMUS will have a standalone momentum resolution of about 20% [10] for low momentum muons. In the upgraded DØ detector we will have charged particle momentum measurement from the Fiber Tracker detector and the SVX: there are at least two central fiber tracker layers up to $|\eta|$=2.0. The overall muon momentum resolution will be significantly better than in Run I, however, the standalone muon track measurement capability will provide better matching of CFT tracks and FAMUS, and will be used in the trigger.

The MDT coordinate resolution has been studied in the test with a 125 GeV/c hadron beam at Fermilab. The 3.5 m prototype has been tested. The Time-to-Digital Converters (TDC) LeCroy 2229 (1 ns time bin) were used for drift time measurements. Only factors connected with inaccuracies in wire position in the tubes, tube position in the plane, and the inaccuracy due to the front-end electronics contributed to the resolution measured in the test beam. The reference system (two multiwire proportional chambers) was used for track position measurement. The distribution of the residuals ($X_{measured}$-$X_{predicted}$) is presented in Fig. 10. The measured MDT coordinate resolution is about 350μm. As it was mentioned above the major contribution to the resolution in Run II is expected to come from drift time

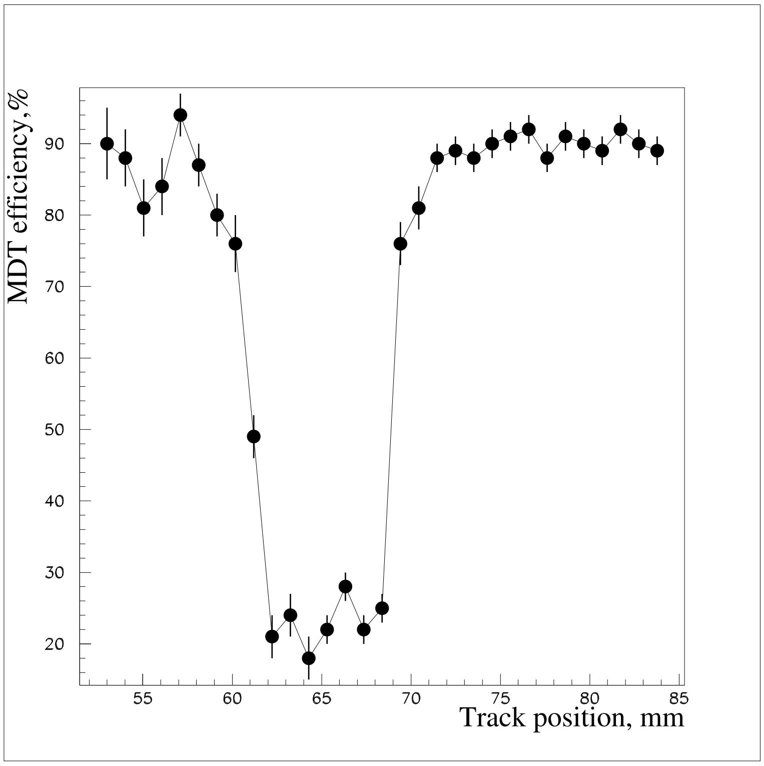

Figure 8: The efficiency of an MDT near the spacers. The spacer size along the wire is 5 mm, but due to electric field degradation in the vicinity of the spacers the inefficient zone is larger.

measurements (the MDT digitizing card uses 18.8 ns time bins) and the alignment accuracy.

3.4 Operating Gas

A good candidate for the fast gas in Run II is the SAMUS gas mixture CF_4-CH_4 (90%-10%). It is non-flammable, fast, exhibits no radiation aging, and a wide operational plateau (Fig. 11), and satisfies safety requirements. All these properties are important for a detector with such number of channels. The working value of the high voltage is about 3100 V. The R-t relation for this gas mixture in the case of the MDTs has been studied in both GARFIELD [14] simulation and at the test beam. Fig. 12 depicts the R-t relation for tracks that are perpendicular to the detector plane. The maximum drift time for 90^o tracks is as low as 40 ns. But even for inclined tracks (at 45^0 angle maximum drift distance is 7 mm) the drift time is below 60 ns. Considering this gas as a baseline choice we continue to look for other less expensive gas mixtures.

3.5 Radiation Aging

Aging tests of MDTs have been performed in Dubna. Several detectors made of original PVC components as well as aluminium combs with stainless steel covers were under study. Fig. 13 presents the single rate and the ratio of signals from the test tube illuminated by a Sr^{90} source and the reference tube without irradiation. The comparison has been done using the signals from a Fe^{55} source. All studies have been performed with the CF_4-CH_4

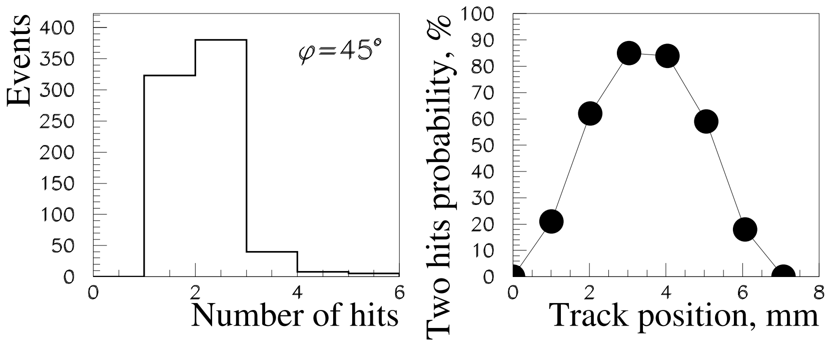

Figure 9: Test beam results for inclined tracks (45^0): The number of hits per plane distribution is shown on the left. Part of event sample had mini-showers so some events have more than 2 hits; The probability of two hits per plane vs. track position is shown on the right.

(90%- 10%) gas mixture and demonstrate no deterioration in the detector performance with accumulated charge up to 1.9 C/cm. The estimated charge accumulated on the anode wires during Run II is about 0.02 C/cm [15]. These studies demonstrate that the MDTs can run for many years at $\mathcal{L} = 2 \cdot 10^{32}$ cm^{-2} s^{-1} without aging.

4 High Voltage System and Electronics

4.1 High Voltage System

We plan to use existing SAMUS High Voltage (HV) system for the MDTs in Run II. In total 48 HV channels will be used (one per octant). Each channel provides HV up to -5kV with the current limit of 2.0 mA. The background measurements [16] and Monte Carlo simulation [17] both show that 2.0 mA is sufficient for operation at the Run II design luminosity. HV from 6 VME type high voltage power supply (Fig. 14) with 8 outputs each via RG58 cables, fanouts and Reinolds cables is applied to fanouts in the collision hall. Most parts of the HV system exist, but 48 RG58 cables with SHV connectors (around 10 m long) to connect the collision hall fanouts with the octants and HV distribution boards inside octants must be provided.

4.2 Front-end Electronics

Each wire of the MDTs is connected to an amplifier and a discriminator located on the octant as close as possible to the signal MDT connectors (to reduce pick-up noise). An Amplifier

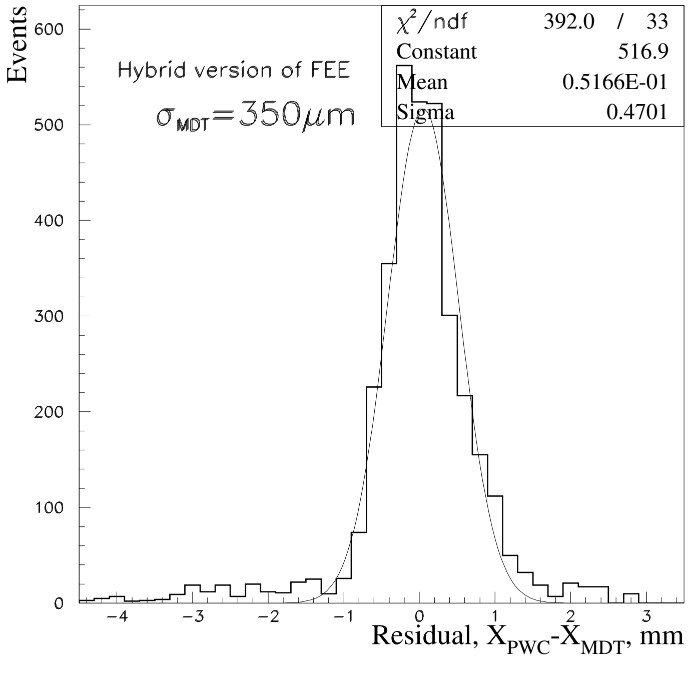

Figure 10: The residual distribution for track positions measured by MDTs and the reference system.

Discriminator Board (ADB) contains 32 channels [18] and provides detection of signals with threshold in the range 0.5-5 μA. Output logical differential signals from ADB are sent via high density flat cables to digitizing electronics situated in VME crates located in the muon trusses. Digitizing electronics accepts logical input signals from the ADB and measure their arrival time with respect to the beam crossing with an accuracy of 18.8 ns. This time bin limits the coordinate resolution of the MDTs. Information from the digitizing electronics is transmitted via serial links to the trigger (hits only) and DAQ (hits and drift time) systems. Details of the MDT electronics system can be found in [18].

5 Gas System

Every plane in each octant will have a separate gas input, and tubes in the same plane will be connected serially. The MDT gas connector design ensures the high hermeticity of all connections and we will, therefore, be able to keep the gas flow at a low rate of 0.5 l/min/octant. Test studies using several MDTs at Fermilab show that this gas flow is sufficient to keep the oxygen fraction at a low level [19].

The gas mixture will be recirculated to save on operating costs. Because the total volume of the MDT is larger than SAMUS's volume by only a factor of two, we plan to use the

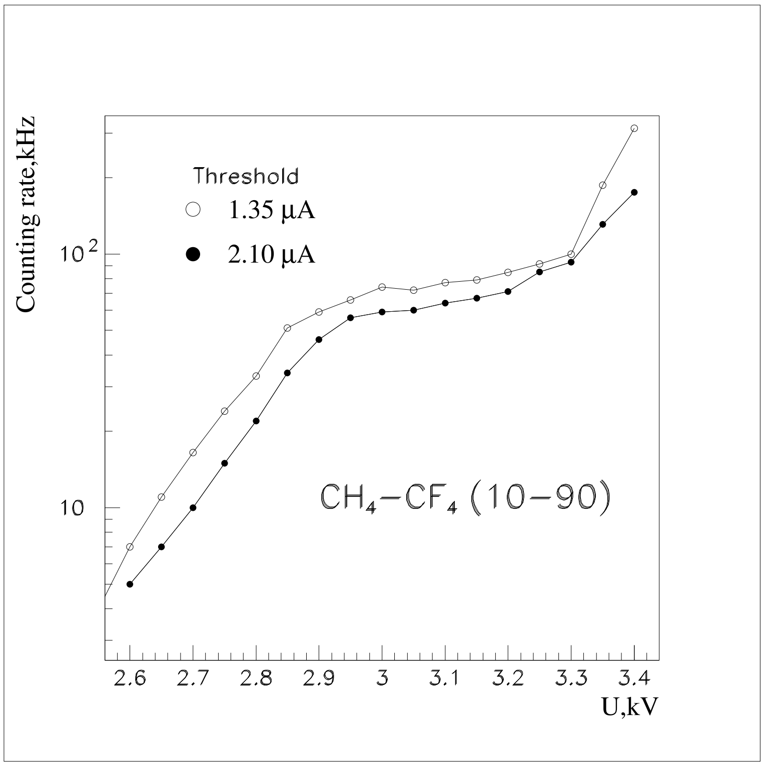

Figure 11: The MDT counting rate vs HV for the CF_4-CH_4 (90%-10%) gas mixture measured in the testbeam.

existing SAMUS gas system with minor modifications.

Input gas pressure and output gas flow will be monitored for each octant. Gas monitoring units and monitor boards from abandoned WAMUS chambers are planned to be re-used. Monitoring of the gas mixture composition will be performed using O_2 and H_2O analyzers and "canary" MDT tubes located in the muon gas room. All gas system monitoring information will be available in real time in the DØ control room using the DØ CDAQ system [20].

6 Alignment and Survey

We are going to use existing DØ experience in the detector survey. All relevant measurements have been done for SAMUS and WAMUS detectors in Run I and it was demonstrated that overall survey accuracy of about 1 mm is achievable. The following steps will be used in the survey procedure:

a) The position of each tube in the plane will be determined by special guides on the assembly table.

b) The octant will have reference tooling balls that will be used to survey the position of every plane in the octant after the octant assembly.

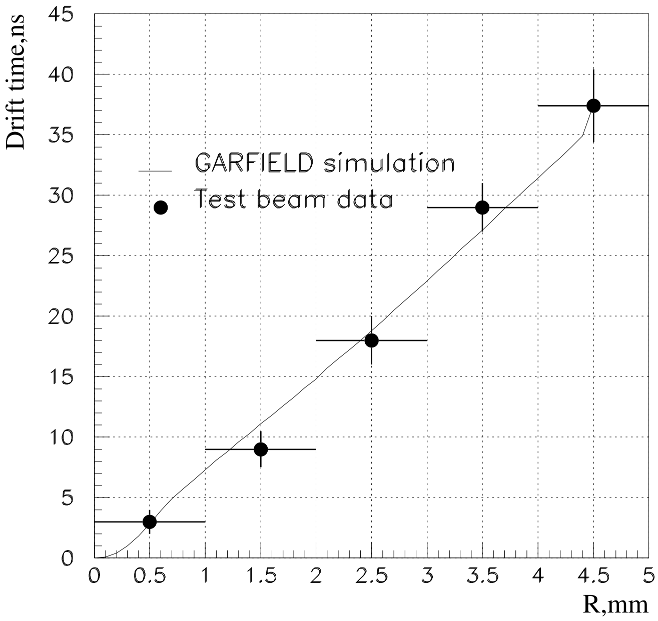

Figure 12: The time-to-distance relation for the CF_4-CH_4 (90%-10%) gas mixture measured in test beam for tracks entering plane with 90^0 angle.

c) The final step of the survey will be to measure the octants position in the collision hall relative to each other and to the DØ coordinate system.

The position of the anode wires inside MDT have been measured in Dubna using so called X-ray tomograph [21]. The 2 m long final design tube was scanned by a narrow X-ray beam. Due to an absorption in the material of the tube, the measured flux of X-rays decreases when the X-rays come through the walls or the wire. This effect allows to locate the wire position with high precision (depending on the accuracy in the X-ray gun position measurement). In Fig. 15 the X-ray picture of the tested tube is presented. The step of the movable table used for these measurements was 20μm. The measured accuracy of the wire location is on average about 160 μm. The results of the test beam measurements confirm that all wires are in their proper positions with the expected accuracy. The expected accuracy of the wire location is presented in Table 3.

7 Assembly and Commissioning

7.1 Mini-drift Tubes Production

The total number of MDT 8-tube modules is 6080 (48640 individual channels). They will be produced at the JINR (Dubna) factory, tested and shipped for final assembly to FNAL.

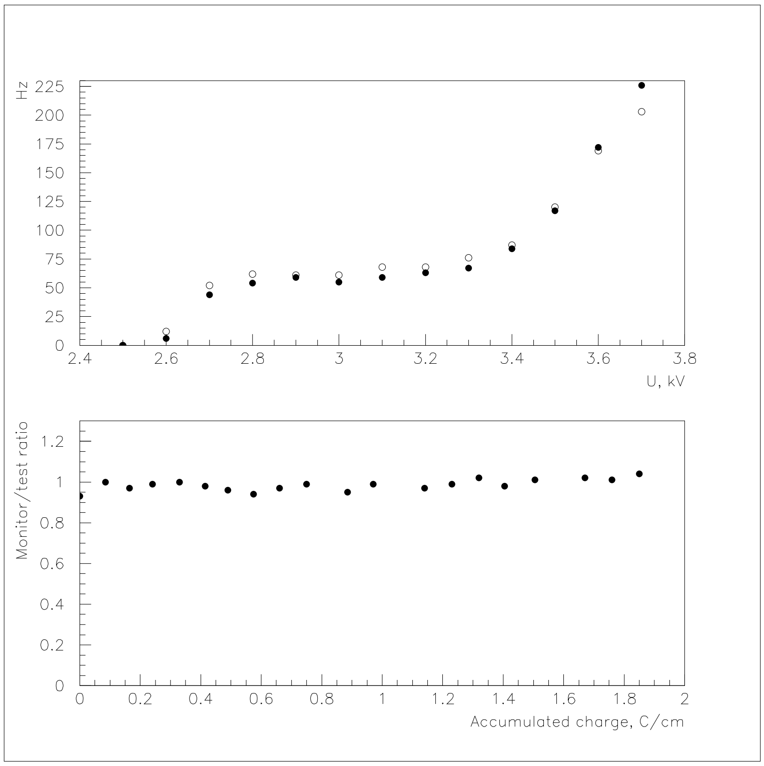

Figure 13: The radiation aging study: the counting rate of the tested (open circles) and reference tubes (black circles) after an accumulation of 1.9 C/cm is shown on top; the signal ratio of tested and reference tubes vs. the accumulated anode charge is presented on the bottom.

The Dubna workshop has a special facility for MDT production and testing. The facility is a large clean hall (680 m^2) with filtered air and over pressure to prevent dust penetration. The aluminium comb is commercially available from Russian industry and has mechanical tolerances of 0.1 mm which satisfies the DØ specifications. The sleeves will be extruded at the JINR workshop. Parts like endcaps, wire spacers, etc. have been made in industry. Before assembly, all the parts pass a thorough cleaning procedure in which all grease and dirt is removed.

In assembly zone, several machines provide the MDT assembly operations. The tube's wiring, soldering at the ends and fixing in the spacers is performed. The fixation of the wire in the spacers is provided by melting the upper part of the spacers. After the wiring combs are inserted into sleeves, the end plugs are sealed by welding them to the sleeve. Fully assembled tubes go to the test procedure.

7.2 Mini-drift Tubes Quality Control

The test procedure includes several tests to be performed immediately after MDT production in Dubna. Those tests are:

- **Gas leak test** - Tubes will be tested for gas leaks by placing them underwater with gas overpressure (about 0.1 atm). The tubes with visible gas leakage will be resealed.

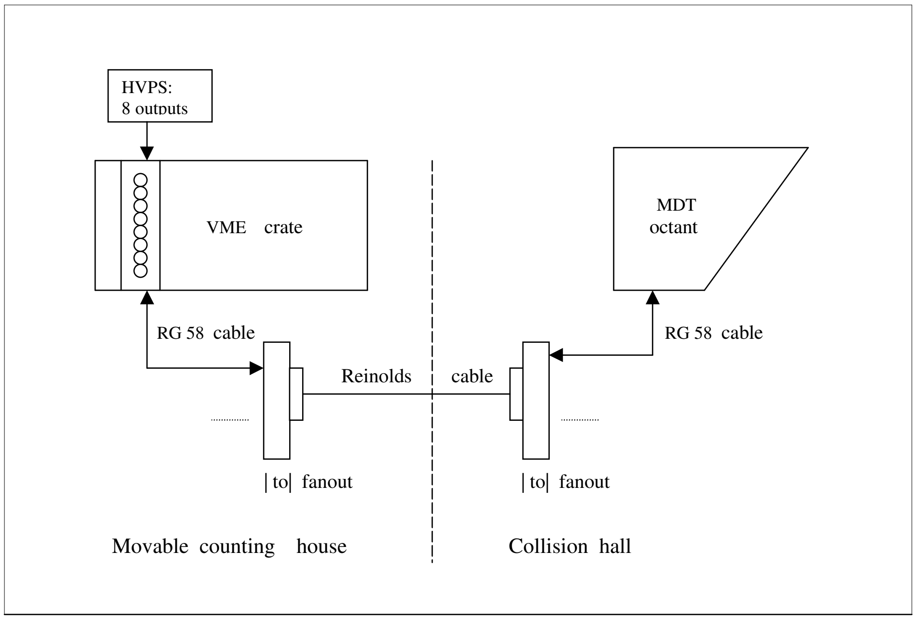

Figure 14: The MDT high voltage system.

Table 3: An accuracy of MDT wire location.

#	Factor contributing into resolution	Accuracy rms(μm)
1	Wire position in the tube	160
2	Tube position in the plane	300
3	Plane position in the octant (survey accuracy)	200
4	Octant position (survey accuracy)	500

- **High voltage test and training** - The high voltage on a batch of tubes is increased by steps up to slightly more than the operational HV. The high voltage is then set at the operational voltage and the tubes remain at this voltage for several hours. The tubes are filled with gas mixture close to the working one. During the HV test the current of all the tubes is monitored and the information is written to the computer. The behaviour of the tubes during the HV test can be monitored and analysed.

- **Signal uniformity test** will be performed using an X-ray gun moving along the wire with simultaneous current control. Fig. 16 depicts a sample of display picture from this test: current vs the X-ray gun position for the 8 wires in the tube. The dip in the middle corresponds to the wire spacer location.

- **Wire tension test** - A sound speaker excites the mechanical vibration of the wires. A high voltage of about 1 kV is applied to the tube. A tube's capacity variation due to the wire oscillation produces an electrical current that can be measured. Resonance frequencies are easily detectable and convert easily into the wire tension.

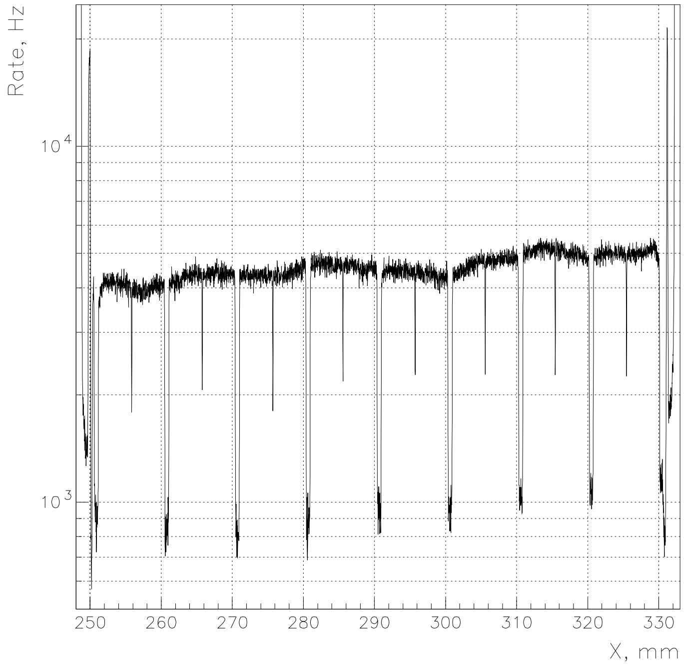

Figure 15: MDT X-ray scan.

After transportation to Fermilab MDTs will undergo the following basic tests: a hermeticity check, a HV test, and, finally, a cosmic ray test of fully assembled octants with front-end electronics.

7.3 Detector Assembly and Commissioning at Fermilab

The MDT octants will be build in Lab F and then transported to the DØ hall for the final installation into the DØ detector. To provide the necessary mechanical accuracy of the planes the following procedure is used for octant assembly. Tables of appropriate size will be built in Lab F. The tables will have special guides to locate the tube supports on the frame. As soon as the position of the supports is fixed on the table, they are welded to the frame, and the tubes can be installed. The support frame is made of aluminium bars covered by aluminium sheets. There are 4 planes in the octants of A-layer, so they consist of two frames with tubes on the each side (Fig. 2). Layers B and C have three planes and the structure is different (Fig. 2).

After the octants assembly is complete the front-end electronics will be mounted on the octant and connected to the DAQ system for the cosmic ray test. The fully assembled octants will be transported to the DAB and installed on the EF toroid (A and B layers) and on the EMC support structure (C layer). After installation all octants will be surveyed, the detectors will be connected to the HV system, the gas system and the DØ DAQ system. Finally, the cosmic muon test will be performed for the whole detector with a final adjustment of operating HV and electronics thresholds.

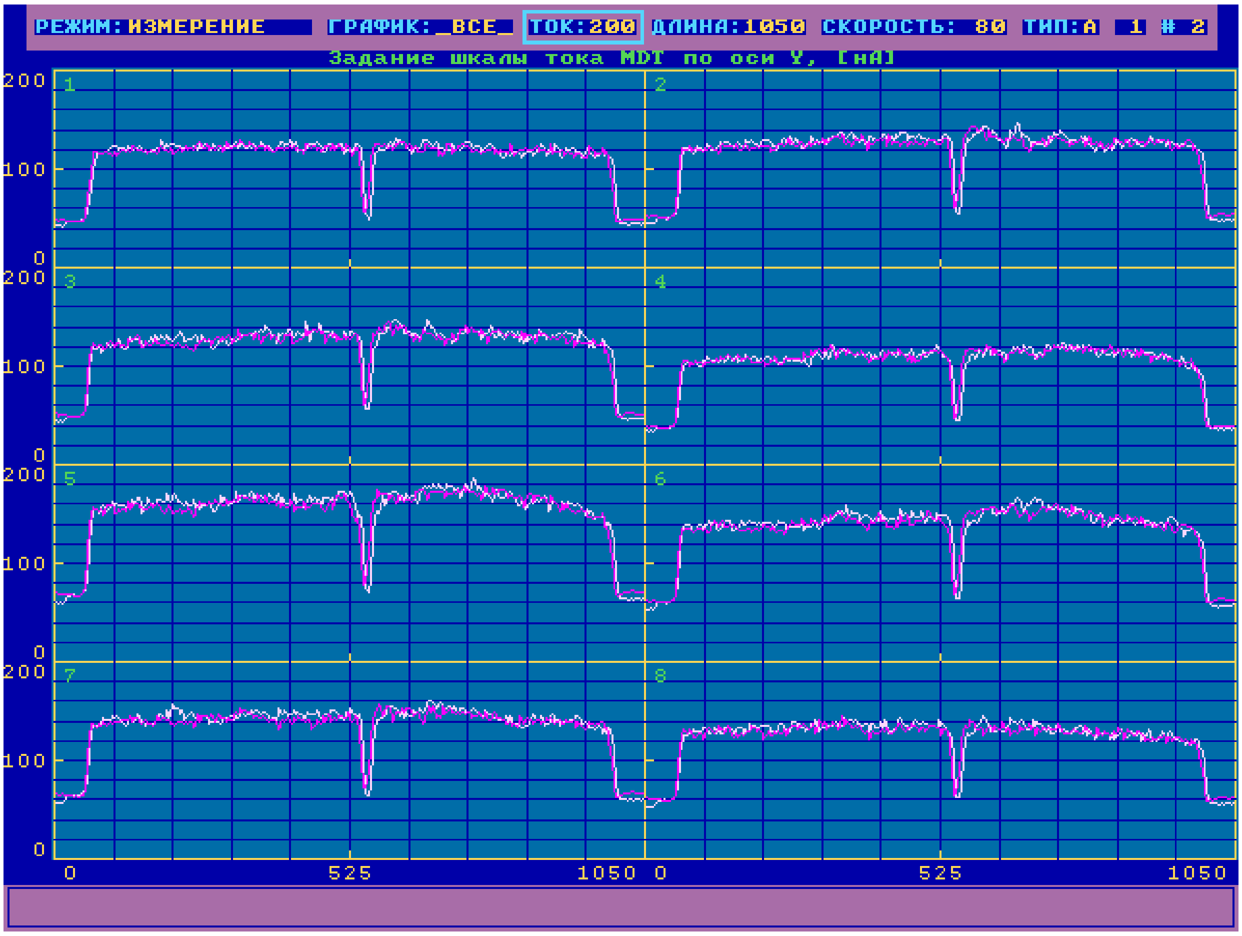

Figure 16: The display of X-ray scan test. Current vs the X-ray gun position for 8 wires of the same tube. The dip in the middle corresponds to wire supports.

7.4 Institutional Responsibilities

Groups of physicists from collaborating institutes will supervise all steps of octant assembly and tests. Responsibilities of each group are specified in the Memoranda of Understanding between Collaborators and Fermilab.

The JINR group is responsible for the MDT design, production, and tests of individual MDT tubes at Dubna, shipment of tubes to Fermilab, and MDT tests after their arrival to FNAL. The JINR group will take part in the supervision of octants assembly, final tests and on-line software developments.

The Fermilab group is responsible for the design of MDT octants, their assembly at Fermilab, installation and survey. The Fermilab group will supervise all steps of the MDT system production and commissioning.

The Northern Illinois University group will participate in tubes tests and take part in on-line software development.

8 Cost Estimate and Schedule

The project cost estimate is shown in Table 4. The project time schedule is shown in Table 5.

9 Conclusions

A well-developed plan exists for construction, testing and commissioning of the DØ forward muon tracking detector based on mini-drift tubes. Prototypes of the final design have been extensively tested and satisfy all requirements. The cost estimate is solid and based on quotes from manufacturers and experience with prototype production. Groups of physicists responsible for the project have been identified among DØ institutions. We see no major obstacles to finishing the project on time for Run II.

References

[1] DØ Collaboration, “The DØ Upgrade”, DØ Note 2542, Fermilab, 1995.

[2] J.M. Butler, “DØ Muon Chamber Pulse Heights: June 1992 to September 1994 Shutdown,”DØ Note 2319, Fermilab, 1994.

[3] R.Jayanti *et al.*, ”The DØ Muon System Upgrade”, DØ Note 2780, Fermilab, 1996.

[4] V.Abramov *et al.*, “TDR for the DØ forward trigger scintillation counters ”, DØ Note 3237,Fermilab,1997.

[5] N. Mokhov, “DØ-SAMUS background simulations”, DØ Note 721, Fermilab, 1988.

[6] J.M. Butler *et al.*, “Reduction of Tevatron and Main ring induced backgrounds in the DØ detector”, FNAL TN-629, Fermilab, 1995.

[7] S. Striganov, “Simulation of the test shielding in the DØ forward muon system”, DØ Note 2711, Fermilab, 1995.

[8] H. T. Diehl, “Aggressive Shielding Strategies for Muon Upgrade”, DØ Note 2713, Fermilab, 1995.

[9] N. V. Mokhov and V. Sirotenko, “Possible Minimal Solutions for DØ Detector Shielding Based on GCALOR and MARS13 Simulations”, DØ Note 2601, Fermilab, 1995.

[10] D.Denisov *et al.*, “FAMUS off line software for Run II”, DØ Note 3244, Fermilab, 1997.

[11] W.Busza “Experience with Iarocci tubes produced on a large scale”, NIM A265, 210, 1988.

[12] G.Alexeev *et al.*,”Studies of stability and systematics of operation of the DELPHI plastic tubes””, NIM A292, 551, 1990.

[13] D.Denisov,"Naming convention for FAMUS", DØ News 1748, Fermilab, 1997.

[14] GARFIELD, a drift chamber simulation program. Version 5.13, CERN, 1995.

[15] D.Denisov, private communication.

[16] D.Denisov, H.Haggerty, private communication.

[17] V.Sirotenko,"Progress on DØ Detector Shielding Optimization with GCALOR", DØ Note 2835, Fermilab, 1995.

[18] A.Khohlov *et al.*, "Muon System Electronics Upgrade TDR", Fermilab, 1997.

[19] J.Norten, "Mini-drift Tube Gas Studies for Upgrade Muon System:Preliminary Performance Results", DØ Note 3278, Fermilab, 1997.

[20] S.Abachi *et al.*, "The DØ detector", NIM, A338 (1994), 185.

[21] L.Vertogradov, "High precision wire positioning measuring in the drift tube package by X-ray scanner (X-tomograph)", ATLAS Internal Note, MUON-NO- 041, CERN 1994; ATLAS TDR 10 (Muon Detector), CERN, 1997, 468"

Table 4: Cost estimate for the Muon Forward Tracking Detector.

Item	Materials (M&S)						
	Unit	**#**	**Unit Cost**	**M&S Total**	**Contingency** %		**Total Cost**
Mini-drift tubes				535,500	15	80,325	615,825
8-Cell Comb	ea	6300	25.50	160,650	15	24,098	184,748
Plastic Sleeve	ea	6300	6.84	43,092	15	6,464	49,556
Stainless Steel Cover	ea	6300	3.30	20,790	15	3,119	23.909
End Cup	ea	12600	4.75	59,850	15	8.978	68,828
Wire Locks	ea	12600	3.45	43,470	15	6,521	49,991
Wire Support	ea	25200	2.15	54,180	15	8,127	62,307
Gas Connectors	ea	12600	3.00	37,800	15	5,670	43,470
Anode Wire	km	151	140.00	21,168	15	3,175	24,343
High Voltage Connectors	ea	6300	6.50	40,950	15	6,143	47,093
Signal Connectors	ea	6300	8.50	53,550	15	8,033	61,583
Mechanical Support				290,016	20	58,003	348,019
Main Support Structure	ea	48	1,100	52,800	20	10,560	63,360
Aluminium Spacers	ea	96	1,021	98,016	20	19,603	117,619
Octants for Mini-drift Tubes	ea	48	2,900	139,200	20	27,840	167,040
Gas System				50,640	20	10,128	60,768
Gas Lines	ea	96	95	9,120	20	1,824	10,944
Gas Connections	ea	48	240	11,520	20	2,304	13,824
Gas Monitoring Devices	ea	4	7,500	30,000	20	6,000	36,000
Signal Cables				94,469	20	18,894	113,362
Signal flat cables (ADB-MDC)	ea	1575	7.5	11,813	20	2,363	14,175
Connectors(ADB-MDC)	ea	1575	10.00	15,750	20	3,150	18,900
Signal cables (ADB-MDC)	ea	6300	2.50	15,750	20	3,150	18,900
Connectors(MDT-ADB)	ea	6300	8.12	51,156	20	10,231	61,387
High Voltage System				157,437	20	31,487	188,924
HV Distribution Boards	ea	6300	10	63,000	20	12,600	75,600
HV Cables	ea	6300	5.25	33,075	20	6,615	39,690
Connectors	ea	12600	4.87	61,362	20	12,272	73,634
Testing and Shipping				30,000	23	7,000	37,000
Test Fixtures	lot	1	10,000	10,000	20	2,000	12,000
Shipping	lot	1	20,000	20,000	25	5,000	25,000
TOTAL FORWARD TRACKING DETECTOR				1,158,062	18	205,837	1,363,899

Table 5: Time Schedule for the Muon Forward Tracking Detector.

Task Name	Duration	Start	Finish
MUON MINI-DRIFT TUBE (MDT) DETECTOR	176.16w	8/1/96	3/2/00
Assembly of MDT modules in Dubna	56w	1/15/98	3/3/99
FULL SCALE ASSEMBLY OF MDT STARTED	0w	1/15/98	1/15/98
Muon Forward Tracker MDT Assembly 10%	0w	4/2/98	4/2/98
Muon Forward Tracker MDT Assembly 50%	0w	8/20/98	8/20/98
Ship modules to FNAL	56w	3/5/98	4/21/99
All Muon Forward Tracker MDT at FNAL	0w	4/21/99	4/21/99
Test of modules at FNAL	52w	5/14/98	6/3/99
FABRICATION OF MDT OCTANTS	160w	8/1/96	10/25/99
Design of MDT octants	36w	7/8/97	4/1/98
SAFETY REVIEW	4w	3/5/98	4/1/98
Assemble Octant Frame	6w	1/15/98	2/25/98
Assemble A,B Layer Supports	12w	5/7/98	7/31/98
Assemble and evaluate Prototype Octant	8w	2/26/98	4/22/98
Prototype MDT OCTANT ASSEMBLED	0w	4/22/98	4/22/98
Final Engineering Design and Drawings for Octants	26w	4/9/98	10/12/98
Procure Materials for Octants Construction	12w	6/19/98	9/14/98
Fabricate Octant Frames	24w	8/17/98	2/17/99
Assemble/Test HV and Signal Cables	26w	7/27/98	2/10/99
Assemble MDT's into Octants	52w	9/15/98	10/4/99
MDT Octant Assembly Begin	0w	9/15/98	9/15/98
Gas System Modifications, Connections and Tests	52w	9/22/98	10/11/99
High Voltage System Connections and Tests	52w	9/22/98	10/11/99
Survey of Assembled Octants	52w	9/22/98	10/11/99
Assemble C Layer Supports	20w	9/15/98	2/17/99
ALL OCTANTS ASSEMBLED	0w	10/11/99	10/11/99
Cosmic Ray Tests	52w	10/6/98	10/25/99

Continuation of Table 5

Task Name	**Duration**	**Start**	**Finish**
INSTALLATION AND HOOKUPS	59.8w	1/12/99	3/24/00
Mount A-layer MDT Octants Onto Supports	4w	2/18/99	3/18/99
Connection to HV System	3w	3/4/99	3/25/99
Connection to Front-end Electronics	3w	3/4/99	3/25/99
Survey of MDT Planes	3w	3/4/99	3/25/99
A-LAYER PLANES INSTALLED	0w	3/25/99	3/25/99
Mount B-layer North Octants Onto Supports	2w	4/22/99	5/5/99
Connection to Front-end Electronics	1w	5/6/99	5/12/99
Connection to HV System	1w	5/6/99	5/12/99
Survey of MDT Planes	1w	5/6/99	5/12/99
B-LAYER NORTH PLANE INSTALLED	0w	5/12/99	5/12/99
Mount C-layer Octants Onto Supports	4w	8/23/99	9/21/99
Connection to Front-end Electronics	3w	9/7/99	9/28/99
Connection to HV System	3w	9/7/99	9/28/99
Survey of MDT Planes	3w	9/7/99	9/28/99
C-LAYER PLANES READY	0w	9/28/99	9/28/99
Mount B-layer South Octants Onto Supports	2w	3/6/00	3/17/00
Connection to Front-end Electronics	1w	3/20/00	3/24/00
Connection to HV System	1w	3/20/00	3/24/00
Survey of MDT Planes	1w	3/20/00	3/24/00
B-LAYER SOUTH PLANE INSTALLED	0w	3/24/00	3/24/00
Cosmic Ray Commissioning	46w	3/25/99	3/2/00
MDT COMMISSIONING COMPLETE	0w	3/2/00	3/2/00
SOFTWARE DEVELOPMENT	78w	3/5/98	9/27/99
On-line Software Development	78w	3/5/98	9/27/99
Creation of Databases	78w	3/5/98	9/27/99
Development of Slow Control System	78w	3/5/98	9/27/99